frontiers in Materials

ORIGINAL RESEARCH
published: 30 July 2020
doi: 10.3389/fmats.2020.00256

On the Variants of Thermal Process in Developing Strong and Ductile Medium Mn Steel

*Shuai Pan and Binbin He**

Department of Mechanical and Energy Engineering, Southern University of Science and Technology, Shenzhen, China

In this contribution, we investigate the influence of three heat treatments, including intercritical annealing (IA), quenching and partitioning (Q&P), and combination of IA and Q&P (IA-Q&P), on microstructure and mechanical properties of the medium Mn steel. The steel treated by the IA process has the largest volume fraction of austenite, which is responsible for the longest elongation and largest energy absorption with the operation of both transformation-induced plasticity (TRIP) effect and twinning-induced plasticity (TWIP) effects. The medium Mn steel produced by IA-Q&P treatment has a mixture microstructure with retained austenite, ferrite, and lath martensite. The existence of martensite in the IA-Q&P steel makes the higher yield strength than that of the IA steel. The better uniform elongation of the IA-Q&P steel than that of the Q&P steel is ascribed to the larger volume fraction of retained austenite and higher mechanical stability of austenite. The Q&P steel has the highest yield stress due to its martensite matrix. It is expected that the tensile properties of medium Mn steel can be tuned by different thermal processes (IA, Q&P, and IA-Q&P) to facilitate its broad automotive applications.

Keywords: advanced high strength steels, martensitic transformation, deformation twins, quenching and partitioning, intercritical annealing, medium Mn steel

OPEN ACCESS

Edited by:
Lijia Zhao,
ArcelorMittal USA LLC, United States

Reviewed by:
Minghui Cai,
Northeastern University, China
Binhan Sun,
Max-Planck-Institut für Eisenforschung GmbH, Germany

***Correspondence:**
Binbin He
hebb@sustech.edu.cn

Specialty section:
This article was submitted to Structural Materials, a section of the journal Frontiers in Materials

Received: *23 May 2020*
Accepted: *14 July 2020*
Published: *30 July 2020*

Citation:
Pan S and He B (2020) On the Variants of Thermal Process in Developing Strong and Ductile Medium Mn Steel. Front. Mater. 7:256. doi: 10.3389/fmats.2020.00256

INTRODUCTION

High-performance steels are desirable to develop lightweight structural components with high safety coefficient in various areas, such as automotive and aerospace. Medium manganese steels are supposed to be a promising candidate of the third generation advanced high-strength steels (AHSS) because of their good mechanical properties, which is ascribed to martensitic transformation during plastic deformation (He et al., 2017; Hu et al., 2017; Liu et al., 2018). Generally, the medium Mn steel is processed by intercritical annealing (IA) to achieve a dual-phase microstructure consisting of ferrite and retained austenite (γ_R) (Lee and De Cooman, 2014; Wang H. et al., 2018; Chandan et al., 2019). The IA temperature and annealing time are crucial to the quantity and stability of the retained austenite (Lee and De Cooman, 2013; Lee and Han, 2014; Han et al., 2015). The amount of retained austenite usually reaches a peak value and then decreases with increasing IA temperature (Gibbs et al., 2011; Ding et al., 2020). Moreover, it is reported that the Mn content in the retained austenite decreases continuously with the ascent of IA temperature, which leads to lower mechanical stability of retained austenite (Lee et al., 2011b). A proper IA temperature can

obtain a large amount of retained austenite with good mechanical stability, resulting in excellent mechanical properties. With longer annealing time, the recrystallization and grain growth of both ferrite and austenite grains will occur, leading to a continuous decrease of yield strength (Han et al., 2015; Ding et al., 2020). Also, it is reported that the volume fraction of retained austenite maintains stable with lengthening annealing time, while the Mn in the austenite phase can increase, which enhances the mechanical stability of the austenite (Han et al., 2015).

Recently, several investigations demonstrate that the medium Mn steel can be fabricated by quenching and partitioning (Q&P) or combination of IA and Q&P (IA-Q&P) processes (Speer et al., 2003; De Cooman et al., 2016; He et al., 2018b). For the Q&P process, a martensite matrix can be achieved by precisely controlling quenching temperature within the range of martensite transform temperature (M_s-M_f) while a certain volume fraction of austenite can be retained through carbon enrichment partitioned from the surrounding supersaturated martensite during the tempering process (Speer et al., 2003; Edmonds et al., 2006). In the conventional Q&P process, the quenching temperature usually deviates from the room temperature, which is challenging to control in commercial continuous annealing lines. To overcome the shortcoming, room temperature Q&P (RT Q&P) concept is recently proposed (He et al., 2018b, 2019; Hou et al., 2018; Kim et al., 2018). By designing the chemical composition of the medium Mn steel, the M_f temperature is reduced below the room temperature and the martensitic transformation is not completed after water quenching. The RT Q&P steel also achieves a good combination of strength and ductility (He et al., 2018b, 2019; Hou et al., 2018; Kim et al., 2018). Compared with the single IA process, the IA-Q&P process can improve the yield strength without sacrificing the elongation (De Cooman et al., 2016). The soft ferrite matrix of the medium Mn steel produced by the IA process is responsible for the low yield strength, while the steel after IA-Q&P process can possess extra martensite, which can increase the yield strength (Cho et al., 2016; De Cooman et al., 2016). Although the medium Mn steel produced by the IA-Q&P process exhibits better ductility than that fabricated by the single Q&P process owing to the optimal mechanical stability of retained austenite, the former has lower yield strength due to the existence of ferrite phase (Wang X. et al., 2018). The mechanical properties of the IA-Q&P steel can be tuned by changing the IA temperature, quenching temperature, and annealing duration.

Although many investigations have reported the microstructure and properties of the medium Mn steel by one of the three thermal processes, the detailed comparison on the microstructure and properties of the same medium Mn steel designed by the above thermal processes has not been conducted. In this contribution, a typical medium Mn steel (Fe-10Mn-0.2C-2Al-0.1V in wt.%) is treated by different thermal processes, including IA, IA-Q&P, and Q&P processes. The microstructure and mechanical properties of the treated medium Mn steels are compared and discussed. It is found that the steels produced by individual IA and Q&P processes demonstrate high yield strength and good ductility. Nevertheless, the steels fabricated by combining IA and Q&P processes show the highest work hardening rate and ultimate tensile strength due to the high quantity of austenite with proper stability. Therefore, depending on the requirement of service in the automotive industry, the medium Mn steels can be treated by different thermal processes to meet the target of weight reduction and safety coefficient.

EXPERIMENTAL PROCEDURE

The investigated steel in this study has a nominal chemical composition of Fe-10Mn-0.2C-2Al-0.1V (in wt.%). The ingot was cast and forged to produce strips with 12 mm in thickness. A homogenization at 115°C for 2 h is performed on the forged strip, followed by hot rolling down to 4 mm in thickness. The hot rolled sample is cold rolled to a 50% reduction after soft annealing at 650°C for 10 h. The tensile specimens with gauge dimensions of 25 mm × 6 mm × 4 mm are fabricated by wire cut along the rolling direction. The variants of a thermal process employed in the present investigation are schematically illustrated in **Figure 1**. The tensile samples are intercritically annealed (IA) at 680°C for different durations, ranging from 10 to 240 min, which are termed as "IA" steels for brevity (**Figure 1A**). The IA temperature is chosen as 680°C because various temperatures in the range of two-phase region were conducted and the mechanical properties of the steel annealed at 680°C are found to be the best. The annealing temperature of tensile specimens are 800°C or 900°C for 10 min and then the samples are water quenched down to ambient temperature (∼25°C) and finally subjected to partitioning at 350°C or 400°C for 10 min (**Figure 1B**). The samples annealed at 800°C are named "IA-Q&P" steels and those annealed at 900°C are termed as "Q&P" steels. Note that the annealing at 800°C is near A_{c3} (**Figure 1B**), which has been reported to have excellent mechanical properties (Cho et al., 2016). The quenching temperature for the IA-Q&P and Q&P process is down to room temperature, at which the martensitic transformation is still not completed (He et al., 2018b). The tensile measurements are carried out using a universal testing machine under a crosshead speed of 1.2 mm/min at ambient temperature. The microstructure of the present steel produced by varied thermal processes is characterized by scanning electron microscope (SEM) and electron backscatter diffraction (EBSD). The distribution of the Mn element in the austenite phase is determined by using energy dispersive X-ray spectrometry (EDS). The SEM and EBSD samples are mechanically polished and then electron-polished in a mixture of ethanol (80%) and perchloric acid (20%) at the voltage of 16 V. The phase evolution before and after the tensile tests is determined by the X-ray diffraction (XRD) measurements (Cu Kα, 1.54056 Å) based on the integrated intensities including (2 0 0) α, (2 1 1) α, (2 2 0) γ, and (3 1 1) γ peaks. The deformation twins in IA steel after the tensile test are observed by using transmission electron microscopy (TEM) in an FEI Tecnai G20. The TEM sample is prepared mechanical grinding down to 0.1 mm, followed by perforation using Twin-jet machine in a solution consisting of 5% perchloric acid and 95% ethanol (vol.%) at −30°C under a potential of 30 V.

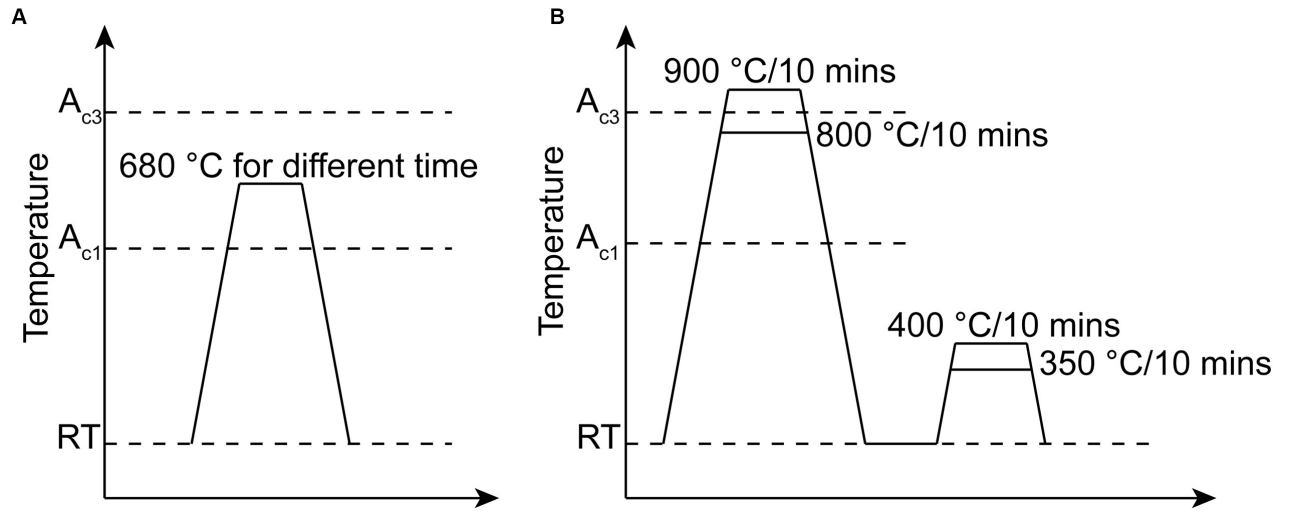

FIGURE 1 | Schematic illustration of the **(A)** IA, **(B)** IA-Q&P, and Q&P processing routes, respectively. RT, room temperature.

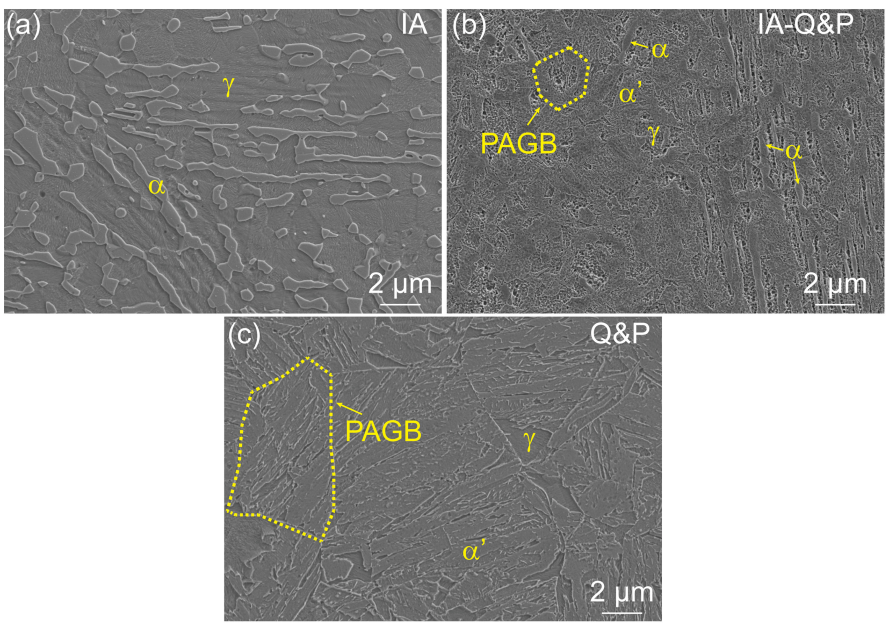

FIGURE 2 | SEM images of the **(a)** IA steel (680°C/240 min), **(b)** IA-Q&P steel (800°C –350°C), and **(c)** Q&P steel (900°C –350°C), respectively. a, ferrite; g, austenite; a', martensite; PAGB, prior austenite grain boundary. The dent part is the austenite. The embossment part is ferrite phase or martensite. The surface of the martensite phase is rougher than that of the ferrite phase.

RESULTS AND DISCUSSION

The IA steel with the annealing time of 240 min presents a dual-phase microstructure with the ferrite located in the austenite matrix (**Figure 2a**). The ferrite grains have both lamellar and granular morphology. The formation of small granular ferrite is the consequence of recrystallization during the prolonged annealing (Han et al., 2015; Ding et al., 2020). The volume fraction of retained austenite is about 64.7% according to the XRD measurement. The ferrite phase with granular and lamellar morphologies can also be found in the IA-Q&P steel after intercritical annealing at 800°C (**Figure 2b**). The prior austenite grain boundaries (PAGBs) can be obviously detected and the average prior austenite grain size is about 1.7 ±0.8 μm. The lath martensite and small austenite can be detected (**Figure 2b**). The volume fraction of retained austenite is calculated to be 48.6% according to the XRD measurement. Typical lath martensite and blocky austenite grains are observed in the Q&P steel (**Figure 2c**). No ferrite phase is detected in the Q&P steel (**Figure 2c**), suggesting that the annealing at 900°C is at full

austenitization region. The average prior austenite grain size is about 7.7 ± 2.7 μm, which is much larger than that of the IA-Q&P steel due to the grain growth at the higher annealing temperature. The austenite volume fraction of the Q&P steel is calculated to be 17.6% according to the XRD measurement. The Mn content obtained from the EDS measurements in the austenite phase of the IA, IA-Q&P, and Q&P steel is 10.9 ± 0.2%, 10.6 ± 0.2%, and 10.0 ± 0.2% (in wt.%), respectively. The Mn content in the austenite phase of the IA-Q&P steel is less than that of IA steel because the longer annealing duration of the IA process allows the sufficient Mn partitioning from the ferrite into the austenite (Han et al., 2015). The austenite in the IA-Q&P steel transforms to martensite during the quenching process, leading to the lower volume fraction of austenite at room temperature. The Mn content in the austenite of the Q&P steel is the lowest among the three type steels. The absence of the ferrite phase at the full austenitization temperature leads to the low average Mn content in the austenite. More austenite transforms to martensite during the quenching temperature, resulting in the lowest austenite volume fraction of the Q&P steel. **Figure 3** presents EBSD phase maps and corresponding inverse pole figures (IPF) of different steel grades. The average grain size of ferrite and austenite in IA steel is estimated to be 0.76 ± 0.32 μm and 0.65 ± 0.40 μm, respectively (**Figures 3a,d**). The grain size of austenite in IA-Q&P steel is 0.49 ± 0.27 μm (**Figures 3b,e**), which is smaller than that in IA steel. The Q&P steel has the largest average austenite grain size (1.2 ± 0.6 μm) among the three steel grades. The austenite volume fraction of the IA, IA-Q&P, and Q&P steels obtained from the EBSD measurements is 47.2, 30.3, and 23.1%, respectively. Note that austenite volume fraction obtained by EBSD measurements is different from the one generated from the XRD tests, which may be due to the difference of measured volume between these two techniques.

The mechanical properties of IA steels annealed for different times are presented in **Figure 4A**. The steel annealed for 10 min exhibits the highest yield strength of 1270 MPa but with the lowest elongation of 1.9%. With lengthening annealing duration from 10 min up to 240 min, the yield strength decreases from 1270 to 1730 MPa, and the total elongation increases from 1.9 to 40% (**Figure 4A**). The ultimate tensile strength of the IA steels (1071 ∼ 1275 MPa) remains stable with the change of annealing time. The prolonged annealing time leads to the strong and ductile IA steel. The decrease of yield strength is probably ascribed to the recrystallization of ferrite and the coarsening of both austenite and ferrite grains (Luo et al., 2011). Thus, the IA steel annealed for 240 min exhibits the best ductility. The tensile curves of the steels annealed for 30 and 60 min show a huge Lüders type deformation. For the steels annealed for 120 and 240 min, the Lüders strain reduces while obvious stress serrations can be detected, suggesting the occurrence of dynamic strain aging during plastic deformation (Zhang et al., 2013). Different from the yield drop detected in the tensile curves

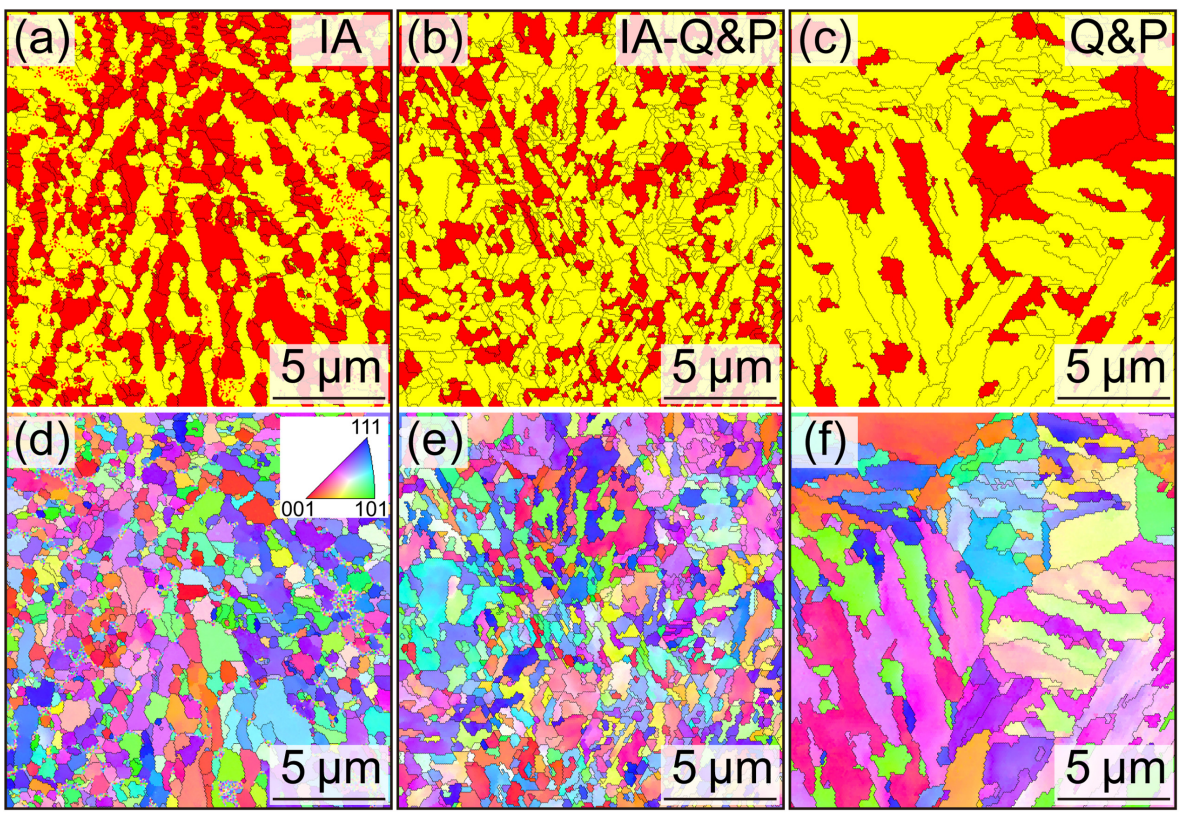

FIGURE 3 | EBSD phase maps and IPF maps of **(a,d)** IA, **(b,e)** IA-Q&P, and **(c,f)** Q&P steels, respectively.

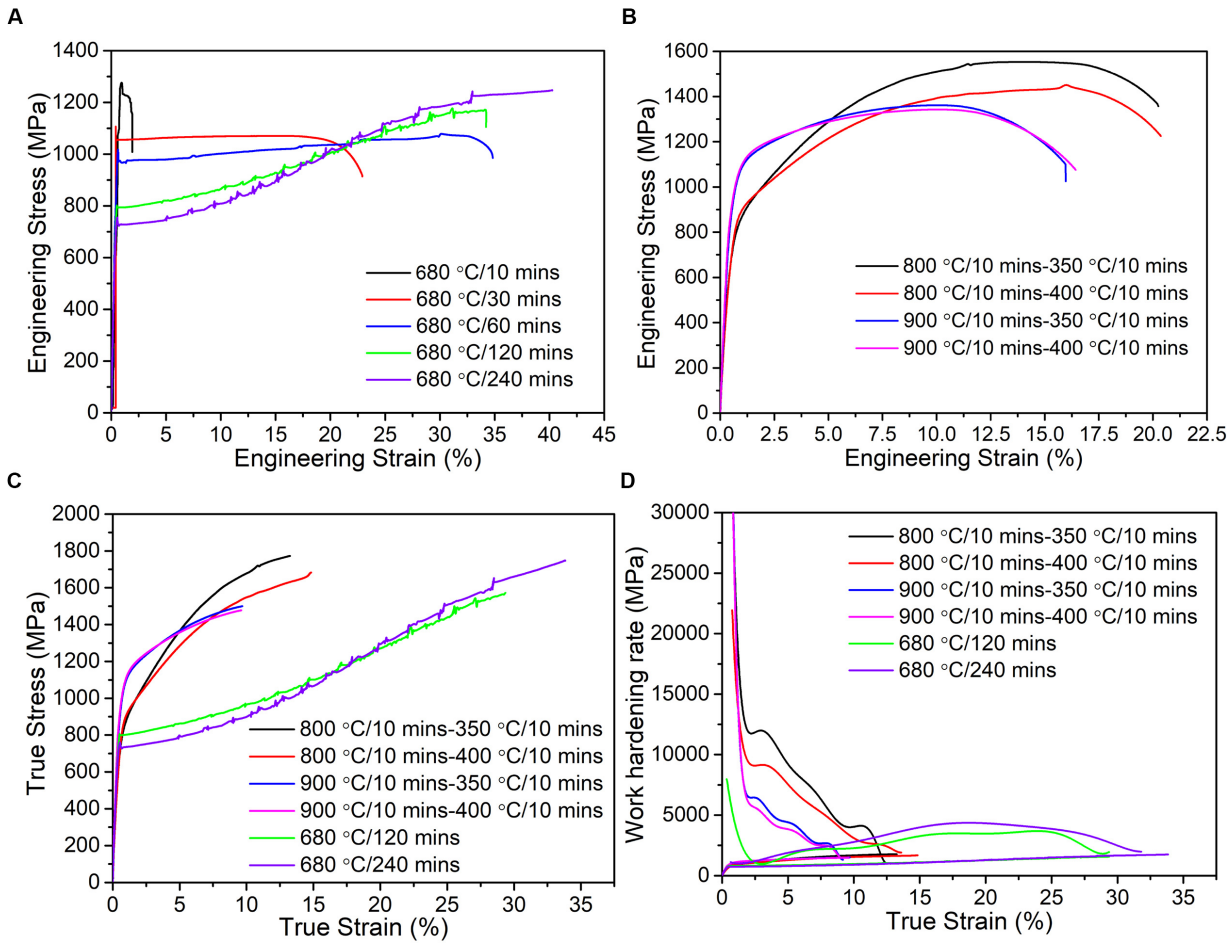

FIGURE 4 | (A) Engineering stress-strain curves of IA steels with different annealing time. **(B)** Engineering stress-strain curves of IA-Q&P and Q&P steels with different partitioning temperature. **(C)** True stress-strain curves of IA, IA-Q&P, and Q&P steels. **(D)** Work hardening rate of IA, IA-Q&P, and Q&P steels.

of the IA steels, IA-Q&P, and Q&P steels present continuous yielding without Lüders band deformation (**Figure 4B**). The yield strength of the Q&P steels (∼ 1 GPa) is higher than that of IA-Q&P steels (810–856 MPa), while ultimate tensile strength and total elongation of the Q&P steels are lower than those of the IA-Q&P steels (**Figure 4B**). The mechanical properties of the steels with different thermal processes have been summarized in **Table 1**. The energy absorption has also been calculated and the IA steel with the annealing time of 240 min shows the largest energy absorption. **Figure 4C** gives the true stress-strain curves of the selected steels. The IA, IA-Q&P, and Q&P steels demonstrate the longest uniform elongation, the highest true ultimate tensile strength, and the best yield strength, respectively (**Figure 4C**). IA-Q&P steels exhibit the higher work hardening rate than Q&P steels until necking takes place, while the work hardening rate of the IA steels is the lowest at the beginning of plastic deformation and then increases gradually (**Figure 4D**). After the true strain exceeds about 18%, the work hardening rate of the IA steels decreases with further deformation (**Figure 4D**).

The highest yield strength of the Q&P steel mainly originates from the martensite matrix (**Figure 2c**). In addition, the dislocations introduced into the austenite phase during the martensitic transformation in the quenching process may contribute to the yield strength of Q&P steel. The existence of the soft ferrite phase is responsible for the low yield strength of the IA and IA-Q&P steels (**Figures 2a,b**). The yield strength of the IA-Q&P steels is better than that of the IA steels, which could be ascribed to the formation of martensite. Besides, the recrystallization and grain growth of both the ferrite and austenite grains is another factor for the lowest yield strength of the IA steels (**Figure 4C**). Given that the austenite transforms to martensite during plastic deformation, the variance of the mechanical stability of retained austenite affects the mechanical behaviors of the steels after yielding. **Figures 5A–C** presents XRD patterns of the IA, IA-Q&P, and Q&P steels before and after tensile tests. The intensity of austenite peaks decreases significantly after tensile tests, suggesting the martensitic transformation takes place in all three type steels. The volume fraction of austenite before and after the tensile tests is shown in **Figure 5D**. Compared with the initial volume fraction of austenite, about 91.6% of austenite in the IA steel transforms to martensite after tensile test. The IA-Q&P steel has

TABLE 1 | Mechanical properties of IA, IA-Q&P, and Q&P steels.

	IA					IA-Q&P		Q&P	
	10 min	**30 min**	**60 min**	**120 min**	**240 min**	**350°C**	**400°C**	**350°C**	**400°C**
YS (MPa)	1270	1052	973	793	730	810	856	1004	988
UTS (MPa)	1275	1071	1078	1177	1247	1553	1451	1361	1342
TE (%)	1.92	22.9	34.8	34.2	40.3	20.3	20.4	16	16.4
EA (GPa·%)	2.45	24.5	37.5	40.3	50.3	31.5	29.6	21.8	22.0

YS, yield strength; UTS, ultimate tensile strength; TE, total elongation (%); EA, energy absorption.

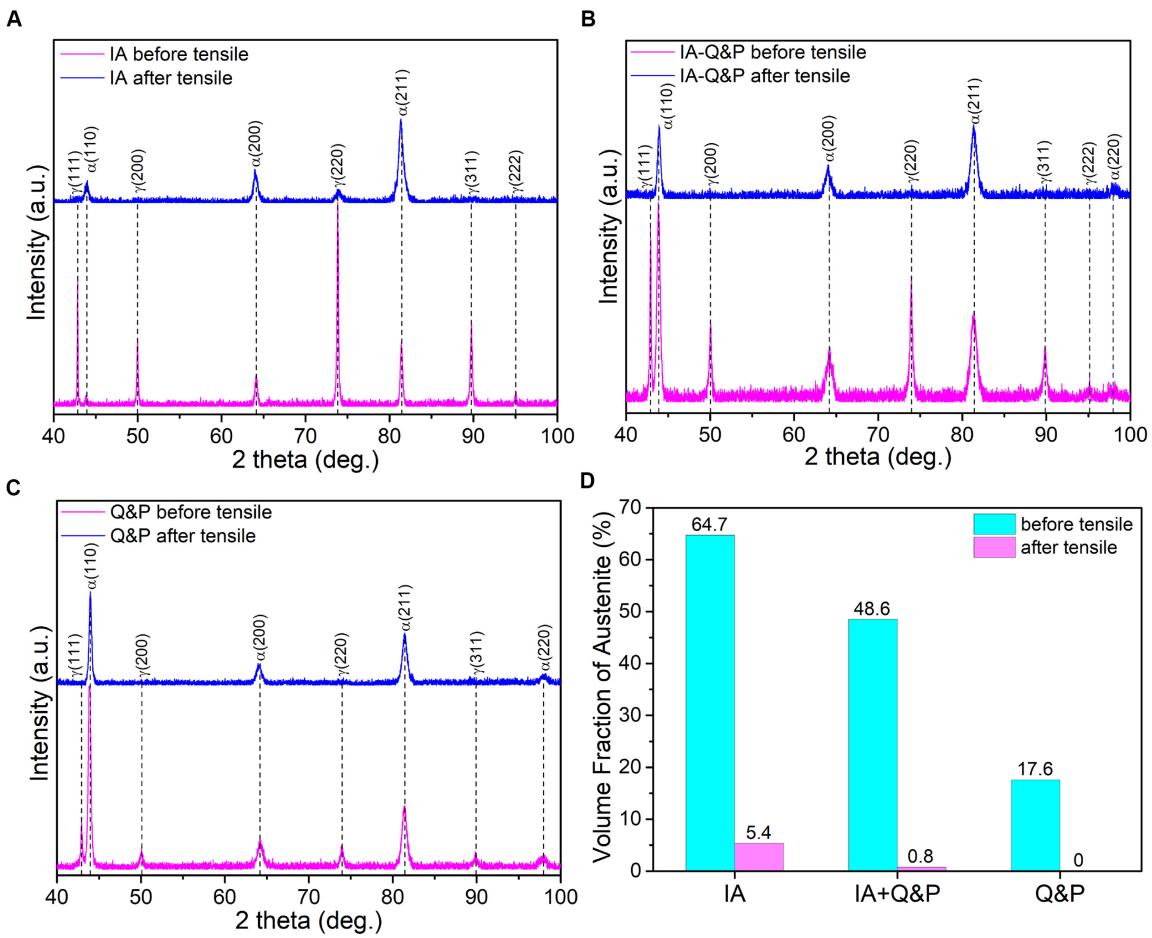

FIGURE 5 | XRD patterns of **(A)** IA (680°C/240 min), **(B)** IA-Q&P (800°C/10 min –350°C/10 min), and **(C)** Q&P (900°C/10 min –350°C/10 min) steels before and after tensile tests. **(D)** The volume fraction of austenite obtained from the XRD measurements. Note that austenite volume fraction in Q&P steel is negligible after tensile test.

a less initial volume fraction of the retained austenite than that of the IA steel (**Figure 5D**). After the tensile test, the volume fraction of retained austenite is only 0.8% and about 98% of retained austenite transforms into martensite. For the Q&P steel, all of the retained austenite transforms to the martensite after the tensile test (**Figure 5D**). The mechanical stability of retained austenite is relevant to the austenite grain size (Jimenez-Melero et al., 2007a,b), chemical composition (Lee et al., 2011; Wan et al., 2019) and dislocation density (Breedis, 1965). The Q&P steels have the largest average austenite grain size (1.2 μm) and the Mn content in the austenite phase (10.0 wt.%) is the lowest. Hence, the austenite in the Q&P steel has relatively low mechanical stability (Jimenez-Melero et al., 2007b; Lee et al., 2011a). All of the austenite transforms to the martensite during plastic deformation for Q&P steel (**Figure 5D**). Owing to the least volume fraction of retained austenite with low mechanical stability (**Figure 5D**), the uniform elongation and the true ultimate tensile strength of the Q&P steels are the poorest (**Figure 4C**). The IA-Q&P steels have the smallest austenite grain size (0.49 μm) and the Mn content in the austenite phase (10.6 wt.%) of the IA-Q&P

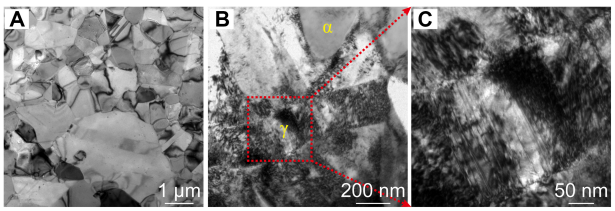

FIGURE 6 | (A) TEM image of the IA (680°C/240 min) steel before tensile test. **(B)** TEM image of the IA (680°C/240 min) steel after tensile test. **(C)** The magnified view of dashed rectangle in **(C)** showing the formation of deformation twinning in the austenite grain.

steels is higher than that of the Q&P steels. So the austenite of the IA-Q&P steels is much more stable than that of the Q&P steels. Although the austenite of the IA steel has the highest Mn content, the austenite grain size of the IA steel is larger than that of the IA-Q&P steel. Besides, both ferrite and austenite phases of the IA steel could have low dislocation density due to recovery and recrystallization during the prolonged annealing process (He et al., 2018a). The austenite of the IA-Q&P steel could have a higher dislocation density because of the short annealing time and the deformation resulted from the volume expansion of martensitic transformation during the quenching process (Greenwood and Johnson, 1965). The austenite in the IA-Q&P steel is expected to be the most stable among the three types of the steels, which leads to the highest true ultimate tensile strength and work hardening rate (**Figures 4C,D**). The higher elongation of the IA-Q&P steel than that of the Q&P steel is ascribed to the larger volume fraction of retained austenite in the IA-Q&P steel (**Figure 5D**).

Regarding the IA steels, the highest initial austenite volume fraction with proper mechanical stability is responsible for the highest elongation (**Figures 4C**, **5D**; Shi et al., 2010). For the IA steel, the Mn content in the austenite phase is the highest one among the different steel grades. In addition, the average austenite grain size of the IA steel (0.65 ± 0.40 μm) is comparable

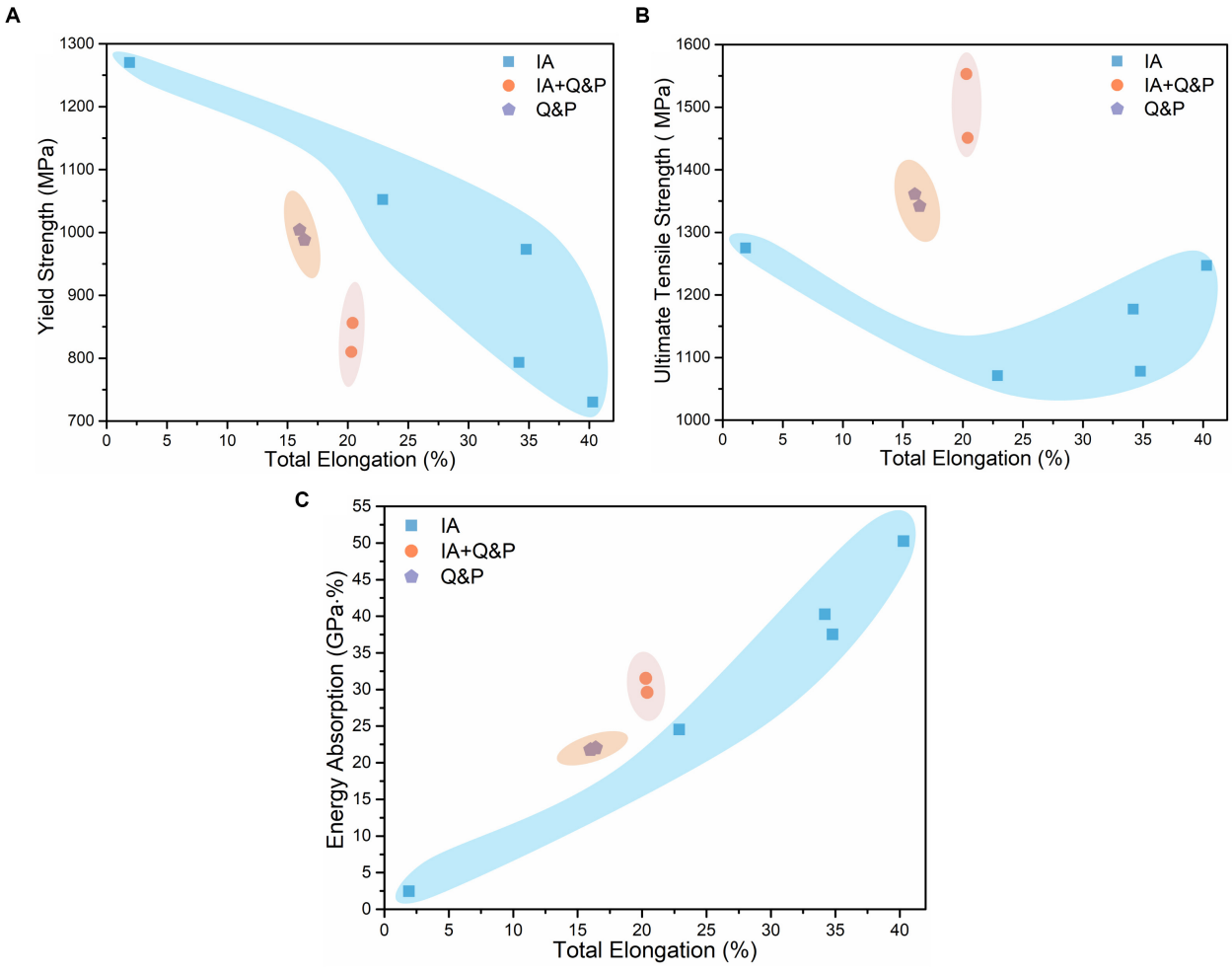

FIGURE 7 | The comparison of tensile properties of the IA, IA-Q&P, and Q&P steels. **(A)** Plot of yield strength against total elongation. **(B)** Plot of ultimate tensile strength against total elongation. **(C)** Plot of energy absorption against total elongation. Energy absorption is defined as the product between the ultimate tensile strength and total elongation.

to that of the IA-Q&P steel (0.49 ± 0.27 μm). Thus, it is expected that the retained austenite in IA steel should has a proper mechanical stability among these three steel grades. The work hardening rate increases gradually after the initial Lüders type deformation (**Figure 4D**), which is related to the transformation-induced plasticity (TRIP) effect during the plastic deformation. However, there is still a small amount of austenite remained after the fracture. As compared to the initial microstructure (**Figures 6A,B**), the dislocation density significantly increases after plastic deformation. Surprisingly, deformation twinning is also found in the untransformed austenite grain (**Figures 6B,C**). According to the EDS measurement, the Mn content in the austenite of the IA steel is the highest (10.9 wt.%) among the three types of steels owing to the sufficient Mn partitioning (Lee et al., 2011; Lee et al., 2011a), which is beneficial for the formation of deformation twins (Grässel et al., 2000; Gibbs et al., 2011). In the present IA steels, the untransformed austenite is those with small grain size, which is more stable than that with large grain size (Jimenez-Melero et al., 2007b). The small austenite grain increases the work hardening rate by forming deformation twinning. The additional twinning-induced plasticity (TWIP) effect also contributes to the increase in work hardening rate (**Figure 4D**). The TWIP + TRIP effect has been demonstrated to efficiently elevate the work hardening rate and thus simultaneously improve strength and ductility of the medium-Mn steels (Lee and De Cooman, 2014, 2015; He et al., 2016).

Figure 7 compares the tensile properties of the IA, IA-Q&P, and Q&P steels. The IA steels possess a better combination of yield strength and ductility with increasing annealing time (**Figure 7A**). The medium Mn steel treated by IA with moderate annealing time or Q&P process is beneficial for the high yield strength and proper ductility, which is desirable for constructing the high strength component such as B pillars in the automobile. The IA-Q&P steels demonstrate the highest ultimate tensile strength among the three types of steels (**Figure 7B**), which provides extra room for weight reduction in structural components where the ultimate tensile strength is the main design criteria. **Figure 7C** presents the energy absorption of the steels. The IA steels exhibit increasing energy absorption with longer annealing time. In general, the IA steels have a better energy absorption capacity than the other two steels, which is suitable for the A-pillar in the automobile. Since the structural components of automotive such as A-pillar and B-pillar require different mechanical properties (i.e., energy absorption, yield strength, and ultimate tensile strength) of AHSSs, it is proposed that the mechanical properties of medium Mn steel can be tailored by utilizing varied thermal processes including IA, Q&P, and IA-Q&P processes to broaden its automotive applications.

CONCLUSION

By systematic tensile tests combined with detailed microstructural characterization, the present work demonstrates that the strong and ductile medium Mn steel can be achieved by varied thermal processes, including IA, Q&P, and IA-Q&P processes. The IA steels have a dual-phase microstructure of austenite and ferrite phases. The IA-Q&P steels possess ferrite and retained austenite together with lath martensite, while the Q&P steel only has martensite and retained austenite. The volume fraction of austenite decreases in the sequence of the IA steels, IA-Q&P steels, and Q&P steels. The IA steels and Q&P steels show a good combination of high yield strength and good ductility, while the IA-Q&P steels have the highest work hardening rate and ultimate tensile strength due to the combination of high quantity and proper austenite stability. The IA steels with prolonged annealing duration have the best energy absorption. Therefore, the present work demonstrates that several variants of the thermal processes are available to design the high-performance medium-Mn steels.

DATA AVAILABILITY STATEMENT

All datasets presented in this study are included in the article/supplementary material.

AUTHOR CONTRIBUTIONS

SP did the experiments and wrote the draft of the manuscript. BH supervised the study and corrected the draft. Both authors contributed to the article and approved the submitted version.

ACKNOWLEDGMENTS

The authors are grateful for the financial support from Start-up Funding from the Southern University of Science and Technology (33/Y01336122). They would like to acknowledge the technical support from SUSTech Core Research Facilities.

REFERENCES

Breedis, J. F. (1965). Influence of dislocation substructure on the martensitic transformation in stainless steel. *Acta Metall.* 13, 239–250. doi: 10.1016/0001-6160(65)90201-4

Chandan, A. K., Bansal, G. K., Kundu, J., Chakraborty, J., and Chowdhury, S. G. (2019). Effect of prior austenite grain size on the evolution of microstructure and mechanical properties of an intercritically annealed medium manganese steel. *Mater. Sci. Eng. A* 768, 138458. doi: 10.1016/j.msea.2019.138458

Cho, L., Seo, E. J., and De Cooman, B. C. (2016). Near-Ac3 austenitized ultra-fine-grained quenching and partitioning (Q&P) steel. *Scripta Mater.* 123, 69–72. doi: 10.1016/j.scriptamat.2016.06.003

De Cooman, B. C., Lee, S. J., Shin, S., Seo, E. J., and Speer, J. G. (2016). Combined intercritical annealing and Q&P processing of medium Mn steel. *Metall. Mater. Trans. A* 48, 39–45. doi: 10.1007/s11661-016-3821-z

Ding, W., Du, J.-C., and Li, Y. (2020). Transformations during intercritical annealing and their implications for microstructure and mechanical properties of medium Mn transformation-induced plasticity steel in continuous

annealing line. *J. Mater. Eng. Perform.* 29, 23–31. doi: 10.1007/s11665-019-04549-3

Edmonds, D. V., He, K., Rizzo, F. C., De Cooman, B. C., Matlock, D. K., and Speer, J. G. (2006). Quenching and partitioning martensite—A novel steel heat treatment. *Mater. Sci. Eng. A* 438-440, 25–34. doi: 10.1016/j.msea.2006.02.133

Gibbs, P. J., De Moor, E., Merwin, M. J., Clausen, B., Speer, J. G., and Matlock, D. K. (2011). Austenite stability effects on tensile behavior of manganese-enriched-austenite transformation-induced plasticity steel. *Metall. Mater. Trans. A* 42, 3691–3702. doi: 10.1007/s11661-011-0687-y

Grässel, O., Krüger, L., Frommeyer, G., and Meyer, L. W. (2000). High strength Fe–Mn–(Al, Si) TRIP/TWIP steels development — properties — application. *Int. J. Plast.* 16, 1391–1409. doi: 10.1016/S0749-6419(00)00015-2

Greenwood, G. W., and Johnson, R. H. (1965). The deformation of metals under small stresses during phase transformations. *Proc. R. Soc. Lond. Ser. A* 283, 403–422. doi: 10.1098/rspa.1965.0029

Han, Q., Zhang, Y., and Wang, L. (2015). Effect of annealing time on microstructural evolution and deformation characteristics in 10Mn1.5Al TRIP steel. *Metall. Mater. Trans. A* 46, 1917–1926. doi: 10.1007/s11661-015-2822-7

He, B. B., Hu, B., Yen, H. W., Cheng, G. J., Wang, Z. K., Luo, H. W., et al. (2017). High dislocation density-induced large ductility in deformed and partitioned steels. *Science* 357, 1029–1032. doi: 10.1126/science.aan0177

He, B. B., Liang, Z. Y., and Huang, M. X. (2018a). Nanoindentation investigation on the initiation of yield point phenomenon in a medium Mn steel. *Scr. Mater.* 150, 134–138. doi: 10.1016/j.scriptamat.2018.03.015

He, B. B., Liu, L., and Huang, M. X. (2018b). Room-temperature quenching and partitioning steel. *Metall. Mater. Trans. A* 49, 3167–3172. doi: 10.1007/s11661-018-4718-9

He, B. B., Luo, H. W., and Huang, M. X. (2016). Experimental investigation on a novel medium Mn steel combining transformation-induced plasticity and twinning-induced plasticity effects. *Int. J. Plast.* 78, 173–186. doi: 10.1016/j.ijplas.2015.11.004

He, B. B., Wang, M., and Huang, M. X. (2019). Improving tensile properties of room-temperature quenching and partitioning steel by dislocation engineering. *Metall. Mater. Trans. A* 50, 4021–4026. doi: 10.1007/s11661-019-05365-z

Hou, Z. R., Zhao, X. M., Zhang, W., Liu, H. L., and Yi, H. L. (2018). A medium manganese steel designed for water quenching and partitioning. *Mater. Sci. Technol.* 34, 1168–1175. doi: 10.1080/02670836.2018.1426678

Hu, B., Luo, H., Yang, F., and Dong, H. (2017). Recent progress in medium-Mn steels made with new designing strategies, a review. *J. Mater. Sci. Technol.* 33, 1457–1464. doi: 10.1016/j.jmst.2017.06.017

Jimenez-Melero, E., van Dijk, N. H., Zhao, L., Sietsma, J., Offerman, S. E., Wright, J. P., et al. (2007a). Characterization of individual retained austenite grains and their stability in low-alloyed TRIP steels. *Acta Mater.* 55, 6713–6723. doi: 10.1016/j.actamat.2007.08.040

Jimenez-Melero, E., van Dijk, N. H., Zhao, L., Sietsma, J., Offerman, S. E., Wright, J. P., et al. (2007b). Martensitic transformation of individual grains in low-alloyed TRIP steels. *Scr. Mater.* 56, 421–424. doi: 10.1016/j.scriptamat.2006.10.041

Kim, D. H., Kang, J.-H., Ryu, J. H., and Kim, S.-J. (2018). Enhancement of tensile properties by room-temperature quenching and partitioning of 0.2C–10Mn–2Al steel. *Mater. Sci. Technol.* 35, 2115–2119. doi: 10.1080/02670836.2018.1522101

Lee, S., and De Cooman, B. C. (2013). On the selection of the optimal intercritical annealing temperature for medium Mn TRIP steel. *Metall. Mater. Trans. A* 44, 5018–5024. doi: 10.1007/s11661-013-1860-2

Lee, S., and De Cooman, B. C. (2014). Annealing temperature dependence of the tensile behavior of 10 pct Mn multi-phase TWIP-TRIP steel. *Metall. Mater. Trans. A* 45, 6039–6052. doi: 10.1007/s11661-014-2540-6

Lee, S., and De Cooman, B. C. (2015). Influence of intra-granular ferrite on the tensile behavior of intercritically annealed 12 pct Mn TWIP+TRIP steel. *Metall. Mater. Trans. A* 46, 1012–1018. doi: 10.1007/s11661-014-2710-6

Lee, S., Lee, S.-J., and De Cooman, B. C. (2011a). Austenite stability of ultrafine-grained transformation-induced plasticity steel with Mn partitioning. *Scr. Mater.* 65, 225–228. doi: 10.1016/j.scriptamat.2011.04.010

Lee, S., Lee, S.-J., Santhosh Kumar, S., Lee, K., and Cooman, B. C. D. (2011b). Localized deformation in multiphase, ultra-fine-grained 6 Pct Mn transformation-induced plasticity steel. *Metall. Mater. Trans. A* 42, 3638–3651. doi: 10.1007/s11661-011-0636-9

Lee, S.-J., Lee, S., and De Cooman, B. C. (2011). Mn partitioning during the intercritical annealing of ultrafine-grained 6% Mn transformation-induced plasticity steel. *Scr. Mater.* 64, 649–652. doi: 10.1016/j.scriptamat.2010.12.012

Lee, Y. K., and Han, J. (2014). Current opinion in medium manganese steel. *Mater. Sci. Technol.* 31, 843–856. doi: 10.1179/1743284714y.0000000722

Liu, L., He, B., and Huang, M. (2018). The role of transformation-induced plasticity in the development of advanced high strength steels. *Adv. Eng. Mater.* 20:1701083. doi: 10.1002/adem.201701083

Luo, H., Shi, J., Wang, C., Cao, W., Sun, X., and Dong, H. (2011). Experimental and numerical analysis on formation of stable austenite during the intercritical annealing of 5Mn steel. *Acta Mater.* 59, 4002–4014. doi: 10.1016/j.actamat.2011.03.025

Shi, J., Sun, X., Wang, M., Hui, W., Dong, H., and Cao, W. (2010). Enhanced work-hardening behavior and mechanical properties in ultrafine-grained steels with large-fractioned metastable austenite. *Scr. Mater.* 63, 815–818. doi: 10.1016/j.scriptamat.2010.06.023

Speer, J., Matlock, D. K., De Cooman, B. C., and Schroth, J. G. (2003). Carbon partitioning into austenite after martensite transformation. *Acta Mater.* 51, 2611–2622. doi: 10.1016/s1359-6454(03)00059-4

Wan, X., Liu, G., Ding, R., Nakada, N., Chai, Y.-W., Yang, Z., et al. (2019). Stabilizing austenite via a core-shell structure in the medium Mn steels. *Scr. Mater.* 166, 68–72. doi: 10.1016/j.scriptamat.2019.03.015

Wang, H., Zhang, Y., Yuan, G., Kang, J., Wang, Y., Misra, R. D. K., et al. (2018). Significance of cold rolling reduction on Lüders band formation and mechanical behavior in cold-rolled intercritically annealed medium-Mn steel. *Mater. Sci. Eng. A* 737, 176–181. doi: 10.1016/j.msea.2018.09.045

Wang, X., Liu, L., Liu, R. D., and Huang, M. X. (2018). Benefits of intercritical annealing in quenching and partitioning steel. *Metall. Mater. Trans. A* 49, 1460–1464. doi: 10.1007/s11661-018-4559-6

Zhang, R., Cao, W. Q., Peng, Z. J., Shi, J., Dong, H., and Huang, C. X. (2013). Intercritical rolling induced ultrafine microstructure and excellent mechanical properties of the medium-Mn steel. *Mater. Sci. Eng. A* 583, 84–88. doi: 10.1016/j.msea.2013.06.067

Conflict of Interest: The authors declare that the research was conducted in the absence of any commercial or financial relationships that could be construed as a potential conflict of interest.